

Quantum  
Magnetics

**N96-185 Man-Portable UXO Detection System:  
Phase I Final Report  
November 4, 1996 – May 4, 1997**

Contract Number: N00164-97-C-0005

by  
Lowell J. Burnett, Ph.D  
Quantum Magnetics Inc.  
7740 Kenamar Court  
San Diego, CA 92121

for  
NAVSURFWARCENDIV  
300 Highway 361  
Crane, IN 47522-5011

QM File Number: CN1309

Distribution approved for public release; distribution is unlimited.

20000508 124

# **Man-Portable UXO Detection System**

## **Abstract**

Existing methods to detect landmines and UXOs depend on inducing an oscillating electric current in the metallic components of the target. For objects with very small metallic content such as plastic-cased mines, these methods have false alarm rates approaching 1000:1. Recently an electromagnetic technique known as nuclear quadrupole resonance (NQR) has been developed to detect explosives directly in their bulk form using radio waves. In the last year, large scale NQR systems have been used to screen airline baggage and mail at airports in the US and Europe.

In this Phase I SBIR program, we investigated the feasibility of modifying current airline NQR systems to make them man-portable and capable of detecting landmines under field conditions. In the context of an overall engineering redesign, we investigated two principal technical issues: 1) the use of advanced signal processing techniques to increase sensitivity and signal discrimination, and 2) the limits of conventional (transistor-based) NQR receivers and the potential improvements offered by superconducting sensors. These studies show that it should be possible to develop a man-portable detection system capable of detecting over 90% of all plastic-cased mines (regardless of metal content) and 100% of metallic-cased mines and UXO when buried at typical depths. We estimate that an NQR-based mine detection system will produce 10 or less false alarms per 100 m<sup>2</sup> at a detection probability of >90%. Phase I successfully sets the groundwork for development and field testing of a prototype NQR-based mine and UXO detector in Phase II.

## **1. INTRODUCTION**

The hazards posed by landmines and unexploded ordnance (UXO) have received considerable attention and publicity in recent years. In fact, they were identified as one of the most difficult problems the US military will face in the 21st century<sup>1</sup>. At the present time, mines and UXO are producing many difficulties for US and UN ground forces in the former Yugoslavia, and have caused several fatalities.

The particular problem to be addressed is the increasing use of "plastic mines". For these the metal content is essentially zero, rendering the mines almost undetectable by existing equipment. The extent of the problem may be grasped by the fact that in the last two years, there have been several international conferences calling for a worldwide ban on the use of plastic mines. To date, no widespread agreement has been reached.

One detectable property of many high explosives is a characteristic, radio frequency emission spectrum when exposed to low power radio waves. This effect is known as nuclear quadrupole resonance (NQR). Starting in the 1970s, efforts were made to develop NQR to find RDX in amounts and at distances typical of antipersonnel (AP) and antitank (AT) mines. Subsequently, there was a concerted effort to improve NQR techniques to detect mixtures of RDX and PETN, which together are the active constituent compounds of plastic explosives. Many technical advances were made, including the development of custom hardware and software that can be operated by low-skilled personnel. These advances have led to commercial development of full size automated NQR systems for checked and carried baggage. In November 1996, the Gore Commission, which was tasked by President Clinton to improve airport security following the loss of flight TWA 800, named Quantum Magnetics as one of five vendors of bomb detection equipment for US airports and airlines.

Nuclear Quadrupole Resonance is the only fundamentally new detection technology to be demonstrated for explosives detection in the last ten years. In comparison with the available technologies used in bomb detection, it is the least expensive and easiest to operate and maintain. NQR is the ideal technique for detecting landmines in that it detects, and *only* detects, the bulk explosive charge, the one component common to all mines. NQR detects the explosive *in situ* without requiring complex sampling techniques. Furthermore, NQR systems are push-button operated, intrinsically simple to maintain, and have the potential to be made fully man-portable. Table 1 lists the particular advantages of NQR for landmine detection. In each instance, NQR has performance superior or equal to other technical approaches such as vapor sensing, X-ray imaging, ground penetrating radar, neutron backscatter techniques, and canines.

**Table 1. ADVANTAGES OF NQR FOR MINE DETECTION**

1. Very high chemical specificity, detection of bulk explosive material in situ
2. True non-invasive detection; no vapor or particulate capture required
3. Immediate, independent repeat measurements are possible for verification of alarms
4. System cannot be saturated by mine signal
5. Red light/green light response. Mine size and depth information possible
6. Very simple to use: commercial systems feature one-button operation
7. Low power RF probing pulses are harmless to humans
8. No consumables or cleaning required
9. Solid state, rugged hardware -- commercial systems achieve > 98% up-time to date

This SBIR program builds on the recent advances made in the development of practical NQR systems for airport use, which have greatly improved the technology since it was last applied to mine detection. In addition, Phase I has been coordinated with a concurrently awarded SBIR Phase I program funded by DARPA, to investigate a *Field Deployable Explosives Detection System*. The goal of this second SBIR program is to compare the relationship between enclosed-volume NQR detection of explosives (as currently employed in airline baggage screening systems) and the single-sided NQR

configuration required to detect explosives in the ground. Information and experimental results of this second Phase I SBIR program have been incorporated in the assessment of the feasibility of the proposed man-portable system.

## **2. PHASE I RESEARCH OBJECTIVES**

Phase I had a single principal technical objective: to carry-out an engineering design study for a man-portable NQR based landmine and UXO detection system for detecting RDX-based explosives. The overall objective was divided into the specific areas of study delineated below:

- 1) Man-portability issues: (expected weight, power consumption and scan rate)
- 2) Alternative signal processing techniques.
- 3) Methods to improve the performance of NQR receiver electronics

Our original Phase I proposal was to consider the feasibility of a detection system to detect *only* the explosive material RDX, which is one of the two principles active constituents of explosives used in landmines. Focusing on RDX detection does not detract from the general goal of assessing a man-portable NQR detector. RDX is a good place to start because it has been the most studied explosive to date, and the same basic methodology used to detect RDX can be applied to the other high explosives used in mines and UXO. However, since we submitted our original Phase I proposal, we have been awarded a substantial contract by DARPA to improve and extend NQR technology, to detect the explosive TNT under the conditions required for a practical mine detection system. The fundamental goal of this new DARPA program is to increase current NQR sensitivity by a factor of three to five and implement the technology in a field system. The overall objective is to develop and demonstrate a man-portable landmine detection system based upon measuring the bulk explosive chemical signature of TNT and RDX using NQR.

Accordingly, we decided to expand the overall (i.e. Phase I + Phase II) program goal. We are now aiming to build a more encompassing NQR system capable of detecting RDX, TNT, PETN and metallic mines and UXO. We expanded the scope of the Phase I study to take into account this increased number of target materials. The overall technical goal and the specific issues to be considered (see above) remained unchanged. However, the feasibility of the proposed system is now evaluated in terms of the complete landmine and UXO detection problem rather than only the subset of targets containing RDX.

## **3. PHASE I RESULTS**

### **3.1 Task 1: Man-Portability Issues**

The fundamental engineering step needed to convert a conventional, enclosed sample-system NQR into a man-portable system for landmine and UXO detection, is to

implement the NQR detection coil in a so-called "single-sided" configuration. To detect an object buried in the ground one must project the radio frequency excitation field and then detect the response of the explosive using an antenna at some standoff from the sample. A "single-sided" coil is a planar coil, often with an electromagnetic shield on one side. It is designed to project the most uniform possible magnetic field into the region on the unshielded side of the coil. QM is a pioneer in developing single-sided magnetic resonance systems, and has built instruments for inspecting aircraft structures and rocket motors. Under the concurrent Phase I SBIR program funded by DARPA, QM has evaluated a group of simple single-sided coil geometries. These results have been used to calibrate our sensitivity for detecting RDX with present NQR technology and methods.

Once the new configuration is implemented, the main issues for man-portability are weight and power consumption. To date, neither QM nor others have seriously attempted to optimize NQR systems to reduce either weight or overall power usage. However, the spin echo NQR approach currently employed uses lower RF excitation power than previous NQR techniques and so represents a step in the right direction.

QM has recently investigated reducing the amplitude of the applied RF magnetic field used to excite the NQR signal. Six months ago, for RDX detection, our 880 liter system used 2 kW peak power to generate a 0.3 mT RF magnetic field with a duty cycle of 20%. To eliminate the possibility of damage to sensitive electronic items that might be in luggage (such as pagers and electronic organizers), we recently reduced our applied magnetic field to 0.06 mT. The input power required is proportional to the square of the magnetic field amplitude. Thus, our peak power is reduced by a factor of around 25, which corresponds to an average input power to the transmitter of around 20W. Unfortunately, we see a concomitant decrease in sensitivity of about 50% on reducing the field to these levels, so there is a trade-off to be made. For PETN, our power levels are presently higher at around 150 W.

For a 25 cm diameter transmitter coil, we need to generate the field in a volume of about 100 liters, which reduces the power needed by  $\sqrt{8.8} \sim 3$ . Hence, it should be possible to use under 50W transmitter power with current NQR technology and methods, and this could be reduced by a factor of two under the DARPA-funded program. The remainder of the NQR electronics is currently housed on two plug-in boards in an IBM-type Pentium computer. The total power budget for these should be under 25 W for an optimized design. A cryocooler will be used to cool the antenna. An input power of <10W should be possible with careful cryogenic design.

The NQR detection coil can be made lightweight since extensive shielding is not required. The largest single contribution to the overall system weight will probably come from the battery pack used to provide electrical power. Lithium batteries provide around 100 W hrs/kg (e.g., 1 W for 100 hours) at 1W per cell (9 cells per kg = 9W power). The Ni-Cd chemical reaction (used in present day rechargeable batteries for laptop computers) provides around 25 W hrs/kg, but at a higher overall power rating of 4 W per cell (7 cells per kg = 28 W power). Thus, even for relatively inexpensive Ni-Cd batteries, an 8 kg

battery pack would be able to provide 50 W of power for about four hours. At this stage, we envision a total prototype weight of about 15 kg. It could be increased if greater time were required in the field; conversely, the weight could be reduced, as operators typically work in one hour shifts.

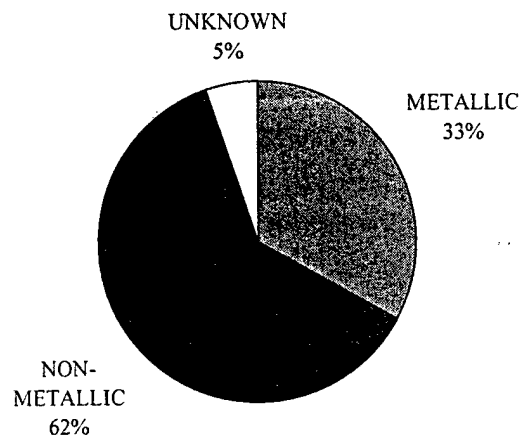
A key area of uncertainty in assessing man-portability is in the wide range of mine types. Specifically, different mines contain different amounts of explosive. We have reviewed the available literature<sup>ii</sup> to find out what fraction of mines have either metal or plastic-cases and (of the plastic mines), what explosives are used, and what fraction of them contain more than 10 g of RDX or TNT and more than 20 g, etc.

The results of this analysis are shown in the following figures. Figure 1 shows the proportion of metallic and non-metallic cases used in landmines. Essentially, all UXO has a metallic case and we find that around one-third of mines are metallic. Figure 2 shows the composition of the explosive charge used in non-metallic mines. The category "unknown explosive" means that the explosive type was not listed for the mine in question. However, we are confident that once the mine surveys are completed the unknown explosive category will turn out to have the same proportion of explosive types as the currently known, i.e. around 90% TNT + RDX.

Our analysis indicates that around 90% of AP and AT mines will be detectable by the proposed TNT+RDX+PETN+Metal detection system. Given the preponderance of plastic mines, the proposed systems represent a dramatic breakthrough in mine detection capability.

Finally, Figure 3 shows the mass of TNT, RDX and PETN present in the mines. This information will be very important in designing and optimizing the proposed NQR system. Generally speaking AT mines contain larger amounts of explosive than we had previously thought.

**BREAKDOWN OF  
CASING MATERIAL  
ANTI-TANK MINES  
(285 mines)**



**BREAKDOWN OF  
CASING MATERIAL  
ANTI-PERSONNEL MINES  
(245 mines)**

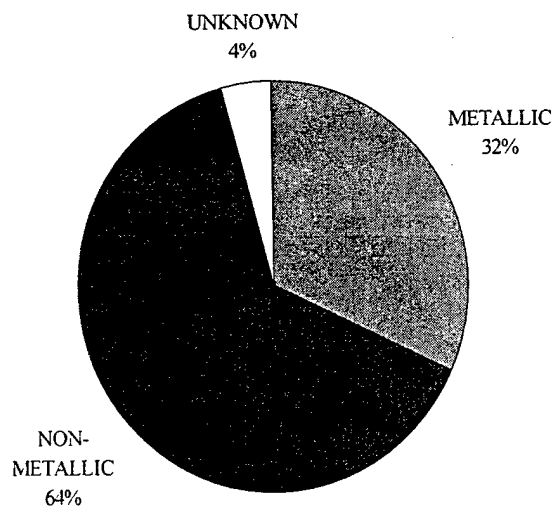


**Figure 1. Casing Material Used in Anti-Tank and Anti-Personnel Landmines**

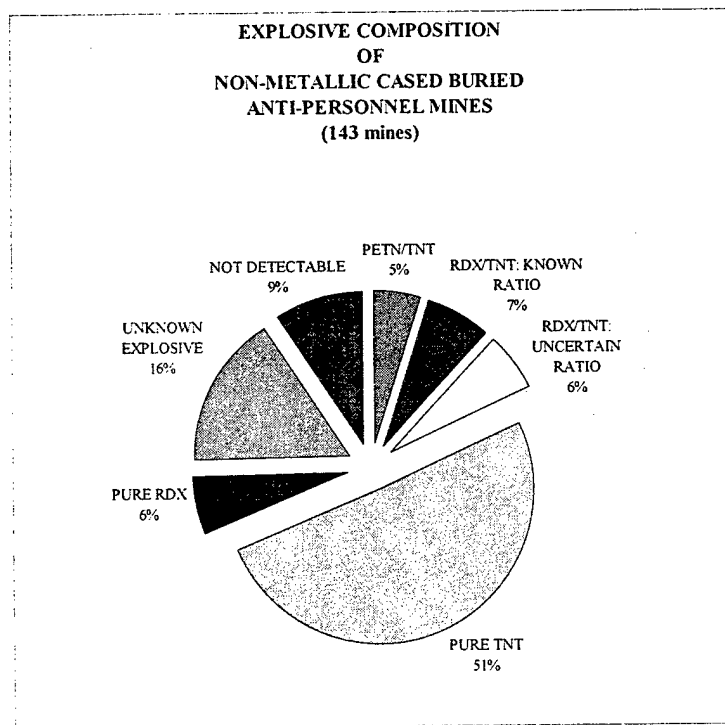
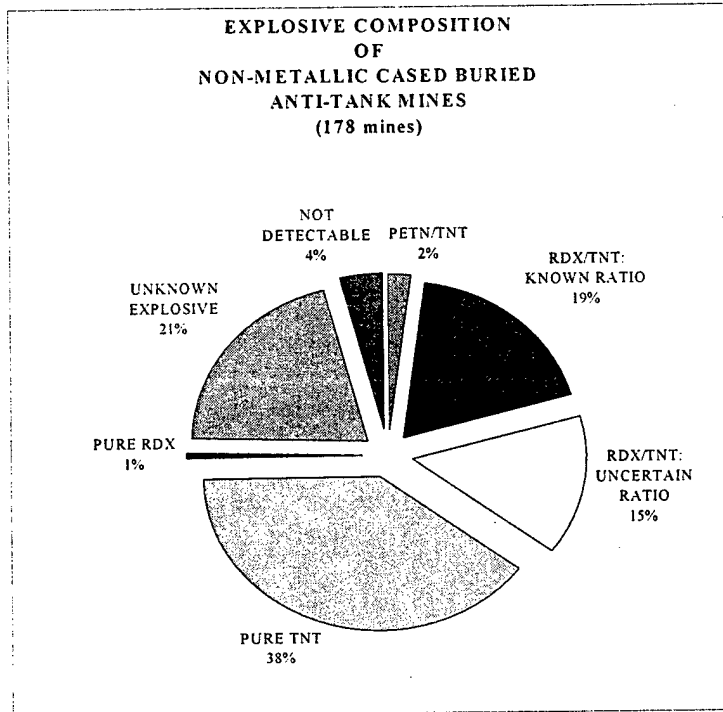
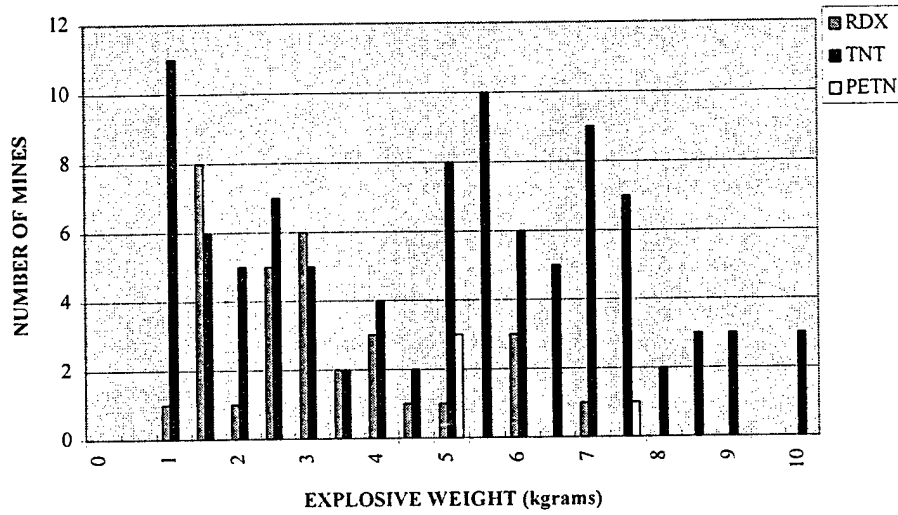


**Figure 2. Explosive Compositions of Non-Metallic Cased Mines**



### NON-METALLIC CASDED BURIED ANTI-TANK MINES



### NON-METALLIC CASDED BURIED ANTI-PERSONNEL MINES

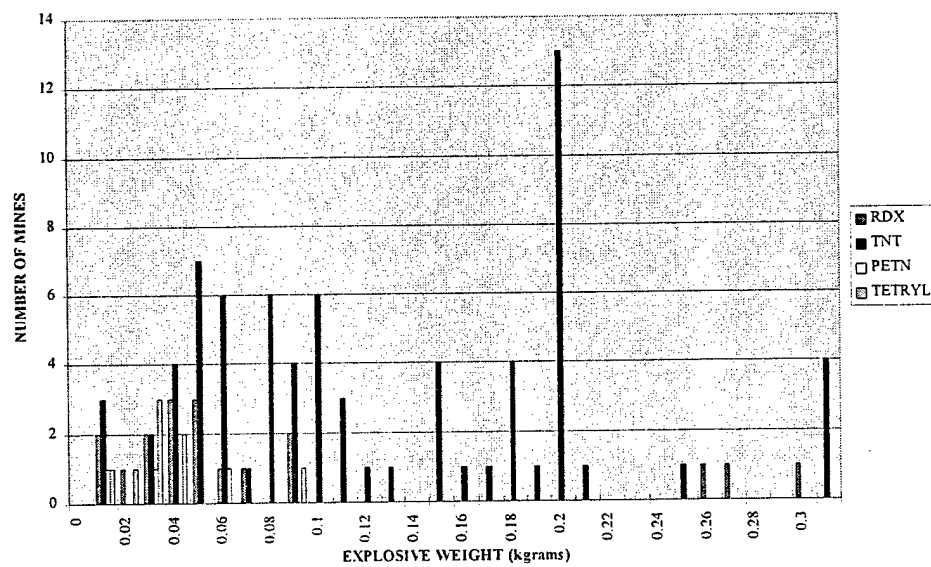


Figure 3. Amount of Explosive Contained in Non-Metallic Mines

### 3.2 Task 2. Signal Processing and Data Acquisition

The San Diego firm of Orincon Inc., is widely known as a leader in the development of advanced signal processing techniques and applications. In particular, it is credited with major advances in acoustic detection of undersea threats and methods so developed are now being applied elsewhere. Orincon has developed a versatile Neural Network (NN) signal processing environment. It is suited to rapid design and optimization of networks tailored for different applications.

QM engaged Orincon as a subcontractor on the Phase I effort, to investigate the utility of NN processing for enhanced detection of RDX, particularly in the presence of interfering signals. The small subcontract has allowed a preliminary study of the problem.

As an initial step, QM furnished to Orincon five data sets representing:

- a) a good RDX signal with little magnetoacoustic ringing (MAR)
- b) a good RDX signal with some MAR,
- c) no RDX signal and no MAR,
- d) no RDX signal with some MAR,
- e) no RDX signal and strong MAR.

This initial set of measurements was designed to give Orincon an opportunity to see what features were present and had to be identified in the data.

Next, approximately 100 different RDX scans were obtained in an airline baggage inspection system. The scans covered a range of RDX amounts from zero to one Threat Quantity of RDX.<sup>iii</sup> The frequency, phase and time evolution of the RDX response are deterministic, and only the amplitude is a statistical random variable. In order to simulate general interference, Dr. Brett Castile of Orincon generated a set of 200 artificial data files with MAR and 200 artificial files of RDX with Gaussian random noise. The parameters for the MAR and noise were based on his observations about the MAR and noise in the initial five data sets. The MAR was modeled as arising from a collection of modes within the NQR excitation band with amplitudes, frequencies, and phases described by random distribution functions. Individual interference data sets were generated using a Monte Carlo method. He then added the interference signals to the randomly scaled versions of the 100 original RDX data sets provided by QM, to generate several hundred simulated data sets. On average for the MAR data sets 24% of the energy was RDX signal, 75% was MAR, and 1% was thermal (Gaussian) noise. For the thermal noise data sets the ratio was 24:1:75 respectively. These two groups comprised the data used for the preliminary evaluation of two alternate processing techniques.

### 3.2.1 Cross-Correlator

The first new technique to be tested was a simple normalized cross-correlator based on a template of the deterministic RDX signal. The cross-correlator was found to give excellent performance in detecting RDX in the presence of Gaussian thermal noise whose coherence with the signal is negligible. An agreement of 97% was achieved between the true average signal to noise ratio and that predicted by the signal processing.

However, due to its very nature, the performance of such a cross-correlator is expected to degrade in the presence of interference with a finite coherence to the template such as MAR. As expected, the normalized cross-correlator performance was lower and the predicted signal indistinguishable from the results of processing data sets with zero RDX signal. However, it should be noted that 75% MAR energy content is much higher than we commonly experience in an actual measurement.

### 3.2.2 Neural Net

Based upon the results of the cross-correlator we applied our second technique, a two layer neural net to the data. The cross-correlator output, together with the Fourier spectral coefficients in the acceptance bandwidth, are used as inputs to a feed-forward NN processor. To make the NN small we chose a limited number of 26 (the real and imaginary components of 13 spectral components), five neurons in the hidden layer, and a single output. There were 130 weights and five biases in the first layer and five weights and one bias in the hidden layer, producing a total of 141 independent parameters to be adjusted during training.

For 141 parameters we need about 300 or more training vectors. Therefore an additional 300 artificial data sets were generated using the method described above. Very little investigation was done on finding the optimal set of basic functions or optimal net architecture for the problem. The process of training is a least squares optimization process and has many local minima. The network was trained several times with additional artificial data sets and each time it settled on a different minimum.

The network performed less well than the cross-correlator. However, this was a simple blind initial experiment and performance is likely to improve substantially with additional effort to find the optimal basis function set and neural net architecture. Also the very high level of MAR is likely to have degraded the detection performance with respect to RDX alone.

### 3.2.3 Neural Net + Cross-Correlator

Two new input vectors were added to the neural net: the real and imaginary parts of the output of the cross-correlator for a total of 28 inputs. The results were better than the previous neural net, but less than for the cross-correlator alone. Only one training of the network was utilized. Additional work is required to determine the potential of this method.

### 3.2.4 Comparison with Signal Processing Currently Used for NQR

To compare the new techniques that were investigated with our present Fourier transform based approach, we collected an additional 100 sets of data with RDX in a commercial NQR detector and 100 with no RDX present (a small quantity of RDX was used so that the ROC curve would have appreciable curvature). Three types of cross-correlator and one neural net architecture were investigated:

Matched Filter Correlator. This is the simplest correlator. The template is the inverse Fourier transform of the five lowest frequency bins found by taking the Fourier transform of the time series data.

Average Correlator. Rather than take the five lowest frequency bins as the template we simply use the average of the time series. This average approximates to the DC value.

Eigenvector Correlator. We use the Eigenvector corresponding to the largest eigenvalue of the data set covariance matrix. Comparison with the other eigenvalues indicates that most of the detection information is projected into this vector.

Feed-Forward Neural Network. The NN inputs were the first 16 eigenvalues of the data covariance matrix. The set of training data was generated artificially, as before (see above).

The performance of these detectors was very similar. We believe that this is due to the very simple nature of the data. Figure 4 and Figure 5 show a receiver operator characteristic (ROC) curves for the Average Correlator, which was the best of the correlators, and for the neural net. In Figure 6 we show the ROC curve derived from the same data set using the signal processing algorithm we have developed for airline bomb detection. We see that for probability of detection (POD) between 70% and 95%, the new methods provide a reduction in the probability of false alarm of about 15% (e.g., for a POD of 90%, the PFA goes from around 45% to 25%).

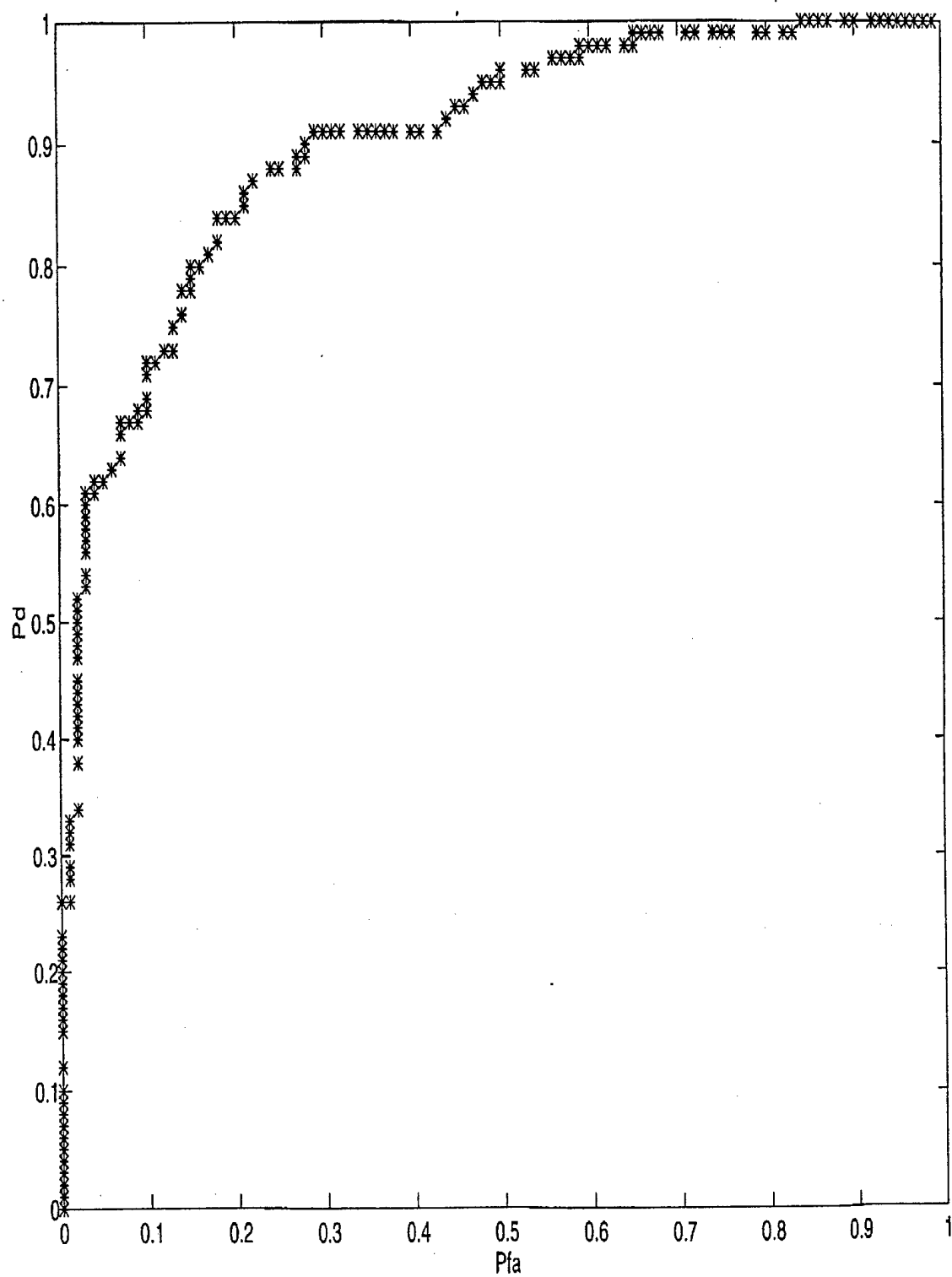


Figure 4. ROC for the Matched Filter Correlator (150g RDX)

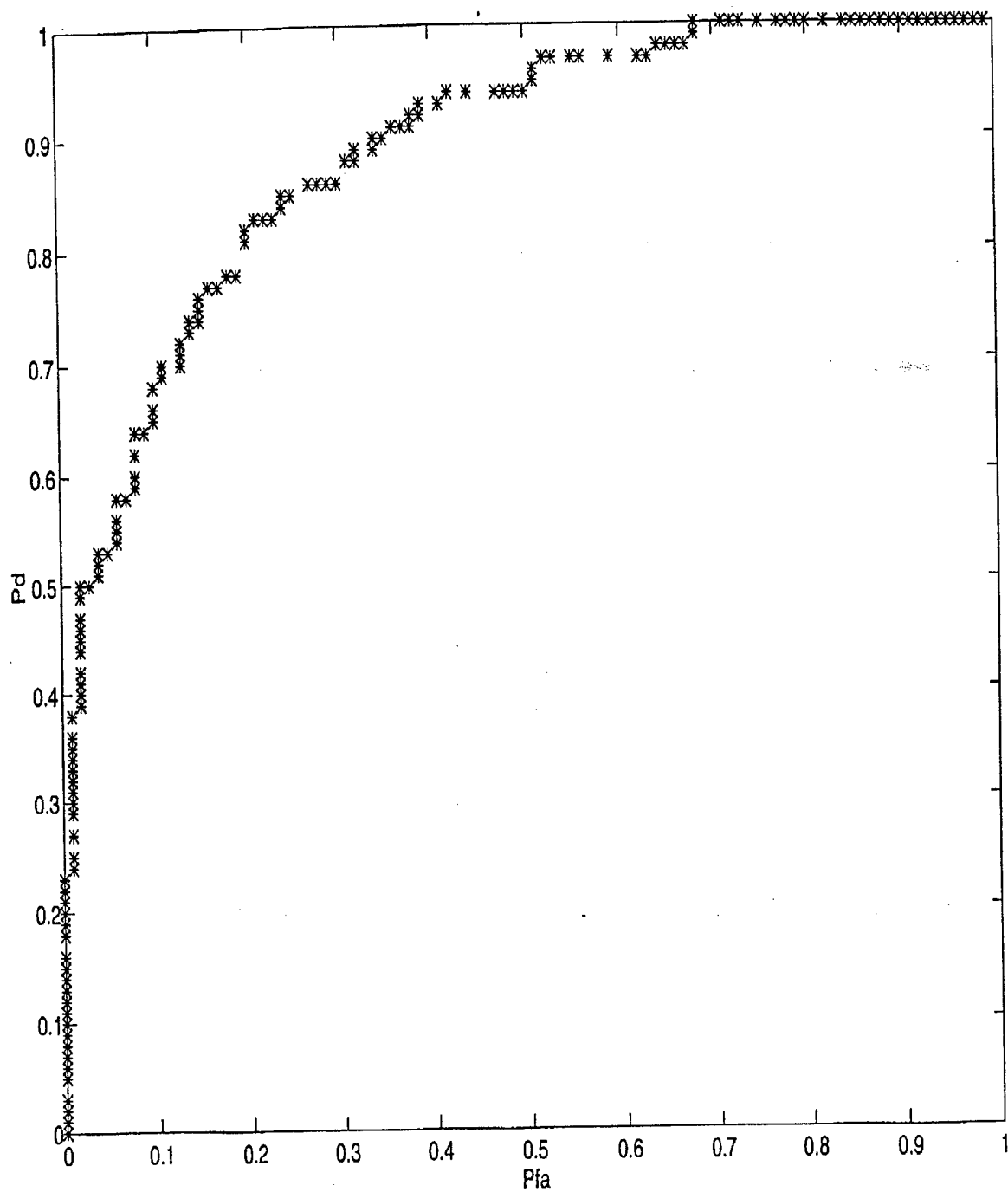
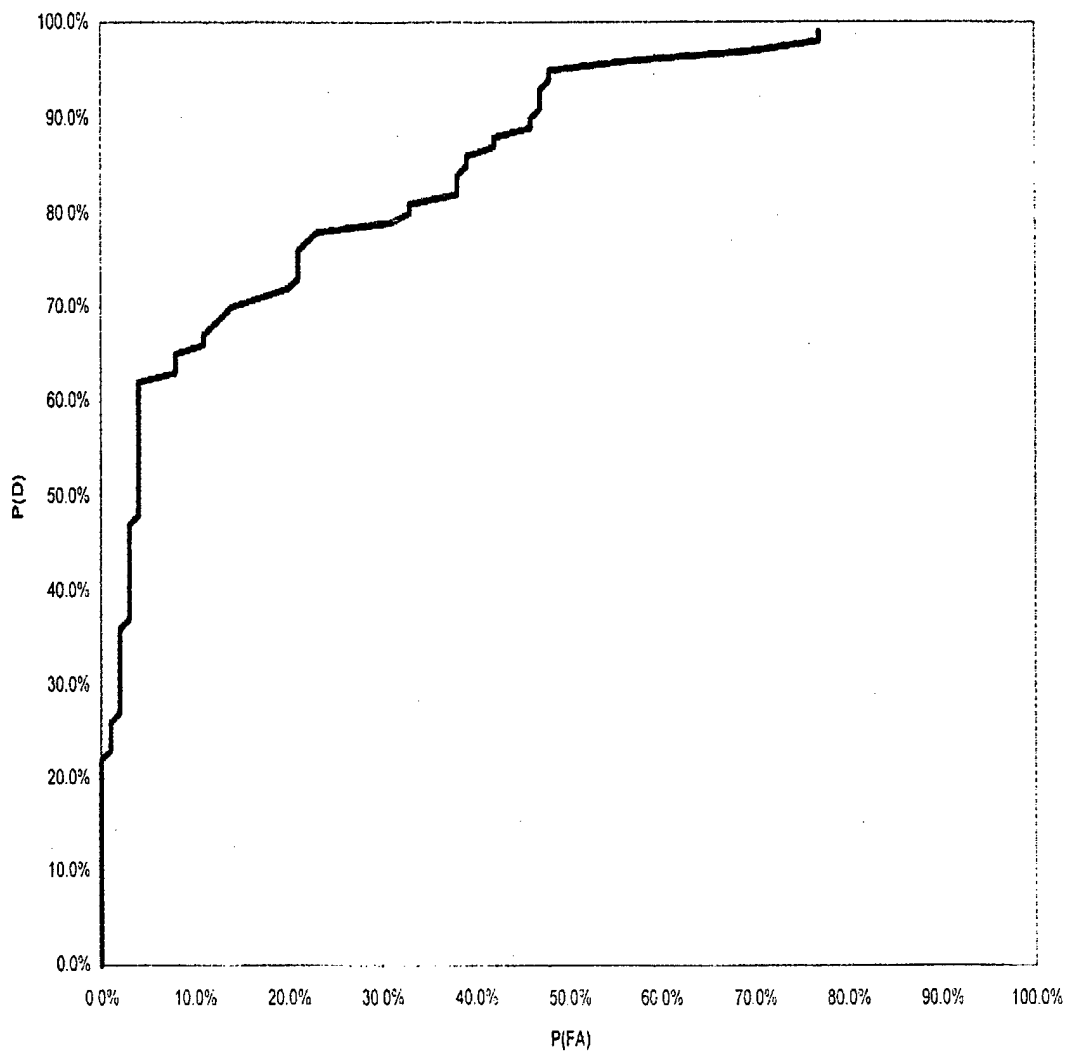


Figure 5. ROC for the Feed-forward Neural Net (150g RDX)

DataSheet Chart 1

Detection of approximately 0.35 threat C4 explosives in QSCAN-1000 3/24/97  
Signal analysis FFT and spike detection only  
Data sets rdx035f and rdxempf



Page 1

Figure 6. ROC Using Current Signal Processing Techniques (150g RDX)

### 3.2.5 Additional Improvements

The new techniques are demonstrably superior to QM's current processing method, which simply sets a detection threshold for a spectral peak within an acceptance bandwidth. However, if there were information separate from the received NQR signals that could indicate the presence of magnetostrictive materials, or at least magnetic metals in the sample volume, it could be used further to improve NN performance. Present NQR devices have to alter their tuning in response to the varying metal content of samples (which alter the electrical impedance of the NQR coil). The degree to which the tuning must be changed is directly related to the amount of metal. This "de-tuning" information could be provided as an ancillary input to the NN. The net can learn the extent of correlation between the metal content signal and the presence of magnetoacoustic ringing, and can thus greatly lower false positives associated with misinterpreted ringing responses.

It may be possible to provide this information via separate, but related measurements. Active mine fields often contain metallic debris (spent shells, shrapnel, discarded food tins, and the like) which may result in magnetoacoustic ringing interference. In addition, certain soils may support piezoelectric ringing responses analogous to magnetoacoustic ringing. Thus, analysis of the effectiveness of NN signal processing to suppress false positives from ringing is highly germane to this program.

Magnetostrictive materials typically possess either remanent magnetization or substantial magnetic susceptibility. In either case, their presence perturbs the earth's magnetic field. A passive magnetometer could detect the presence of magnetic materials and provide yet another ancillary input to the NN. The combination of a metal detection (via coil de-tuning) and magnetic anomaly detection (via passive magnetic sensing at dc) could prove crucial to the ability of a NN to suppress false alarms from magnetoacoustic ringing.

The de-tuning response of the NQR coil also measures soil conductivity. To provide an ancillary NN input to help deal with piezoelectric ringing, one can use a low-cost sensor that measures the dielectric constant of soil. This is analogous to the passive magnetic measurement to assist in identifying potential sources of magnetoacoustic ringing. These and other modifications to the NN approach will be considered in Phase II.

### 3.3 Task 3. Detection Head Electronics

In all current NQR apparatus, the antenna and electronic preamplifier used to detect and boost the NQR signal are currently the limiting factor for detection performance. That is to say, the antenna and preamplifier ("the detection circuit") are the dominant noise sources in the measurement scheme. Under the Phase I program, we investigated two alternative methods to reduce the noise of the detection circuit. The first is to design and develop a custom preamplifier using cooled semiconductor transistors instead of the present room temperature technology. The second alternative is to replace the transistors altogether with a Superconducting Quantum Interference Device (SQUID).



To evaluate these alternatives, it is first necessary to develop a precise model of the physical system to be measured and the gain and noise sources of the detection system. In order to make a reliable comparison, the model must be suitable for use with both semiconductor and superconductor detection electronics. No such model exists in the scientific literature, and so we have had to develop one.

### **3.3.1 Analysis of the NQR Measurement and Instrumentation Problem.**

#### **Limits on the available NQR signal power**

We first need a rudimentary model of the signal source. The NQR signal results from a precession in the orientation of the  $^{14}\text{N}$  nuclei in the target substance that has been excited by an applied RF pulse. As the nuclei precess, their dipole moment generates a small fluctuating magnetic field in the vicinity that can be detected by a pickup loop and amplifier system. The voltage induced in the pickup antenna equals the time rate of change of the magnetic flux that threads the loop.

Because the signal is in the form of an induced voltage, it raises the question, "what is the available signal power that can be coupled via the antenna to the amplifier?" The power available from a signal voltage is determined by the signal's effective source impedance, as seen by the preamplifier. This impedance will be at its lowest when any series reactive terms in the antenna are resonated out, for example, by a capacitor placed in series with the inductance of the pickup loop. Residual resistance in the coil, however, cannot be resonated out and therefore represents a lower limit on the source impedance of the signal and antenna. Because power scales as the voltage squared divided by the impedance, the maximum signal power is available when all the reactance has been canceled out. Although this maximum is only available at resonance there are techniques (to be discussed later) that can broaden the resonance and thereby improve the bandwidth.

The above argument suggests the signal power is only limited by losses in the coil. If a superconducting pickup coil, which has zero resistance, were resonated with a low loss (superconducting) capacitor, it would appear that an arbitrarily large power could be extracted from a given nuclear system. However, this argument breaks down eventually, because the nuclear spin system has only a limited amount of energy that can be extracted. This apparent paradox comes from the fact that the coupling of the nuclear spin system to the pickup loop is usually very weak. In principle, if the quality factor,  $Q$ , of the pickup system were sufficiently large (losses sufficiently low), at resonance the circulating currents in the coil would build to a point where the resulting magnetic fields would directly perturb the nuclear spin system. At this point our model of the NQR signal acting as a fixed voltage source would break down. Nevertheless, until this point is reached it can be seen that as the electrical  $Q$  of the pickup loop increases, the available signal power increases.

In practice, the minimum achievable source resistance in the pickup coil is limited by other factors, and the critical coupling will never be reached. The series resistance of the coil can be made negligibly small by using a superconducting pickup loop. However,

losses will still be coupled into the coil from non-superconducting materials in the vicinity of the coil, including losses in the sample material being scanned. In practice, there will be some limiting  $Q$  of the pickup circuit.

A parameter we are free to change is the number of turns in the pickup coil. For a fixed magnetic signal from the NQR system, the induced voltage will increase proportionally with the number of turns. Such a modification would also affect the coil's reactance, increasing it as the turns squared. Despite any such scaling, the  $Q$  of the pickup coil is largely independent of the number of turns in the pickup loop because the resistive component in the coil also scales as the turns squared. The maximum available signal power, which scales as  $V^2/R$ , will therefore be independent of the number of turns and be determined only by factors such as the  $Q$  of the pickup coil, and geometric parameters such as the volume of the pickup coil and the volume of the sample.

#### Noise analysis of a simple detector circuit.

The two dominant contributions are thermal noise in (or induced in) the pickup coil and the noise of the following amplifier. A simple circuit model for a pickup coil connected to an amplifier is shown below. The signal voltage is represented by  $V_{sig}$ .  $V_{nt}$  represents the thermally excited Nyquist noise voltages that arise from dissipation in the coil. Noise contributions from the amplifier are shown as two separate sources,  $V_{na}$  and  $I_{na}$ . These will be described in more detail shortly. The capacitor  $C1$  is used to resonate the coil, while  $C2$  is used to match the antenna to the amplifier.

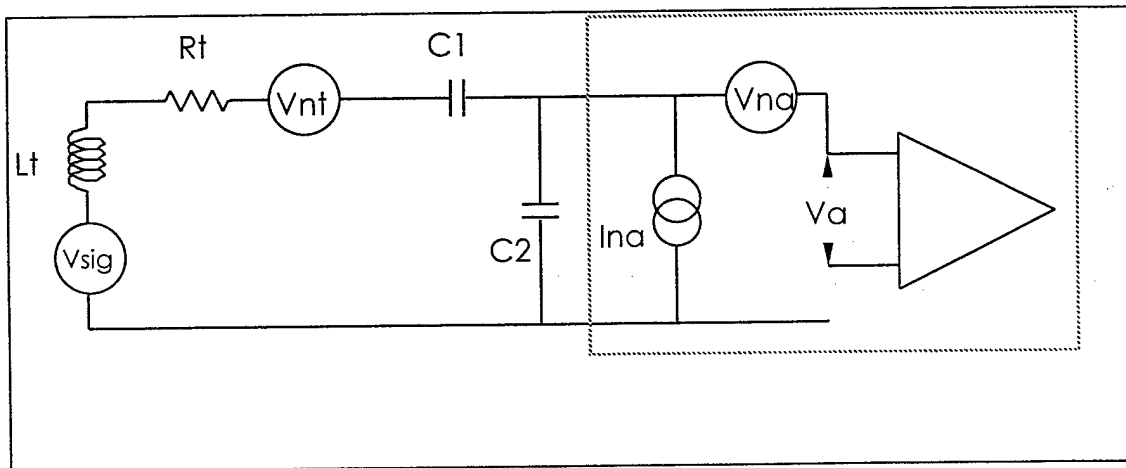


Figure 7. NQR Detection System Circuit Model for Noise Analysis

$V_{nt}$ , the thermal noise, derives from a fundamental noise mechanism described in statistical mechanics by the 'fluctuation-dissipation' theorem. The theorem ties dissipation, the conversion of 'motion' to heat, to a reverse process where a thermally generated random 'force' drives a fluctuating 'motion'. Both dissipation and thermally driven fluctuations are inseparable and a direct result of the coupling of a system to the thermal bath through a dissipation mechanism. In our case the 'motion' we are talking of

is the flow of current through the circuit, the dissipation mechanism is the electrical loss in the coil, and the random force is a thermally excited noise voltage.

To model the noise in an amplifier, it is common to separate the model into an ideal, infinite input-impedance noiseless amplifier with coupled noise sources on the input. A finite input impedance for the amplifier could also be included in this model by placing its impedance in parallel with  $C_2$ , though we ignore this here.

The voltage noise term  $V_{na}$  represents a noise that adds directly to the voltage presented to the amplifier input. The current noise term  $I_{na}$ , represents a noise current from the amplifier that flows back through the input circuit. This noise current induces a noise voltage across the input circuit that depends on the circuit impedance as seen from the amplifier. Any realistic amplifier model must include both contributions. Without both it would (in principle) be possible to connect a transformer to the input, and scale any input signal arbitrarily above the noise.

All the noise terms discussed above can be combined into one expression in order to show the way they combine and appear at input to the ideal noiseless amplifier. This gives the following expression ( $\omega$  is the angular frequency =  $2\pi.f$ )

$$V_a(\omega) = V_{na}(\omega) + I_{na}(\omega) Z_m(\omega) + (V_{sig}(\omega) + V_{nt}(\omega)) \frac{X_{C2}(\omega)}{Z_l(\omega)}$$

where  $V_a(\omega)$  = the voltage presented to the noiseless amplifier input  
 $Z_m(\omega)$  = the impedance of the input circuit as seen from the amplifier input  
 $Z_l(\omega)$  = the impedance of the input circuit as seen from  $V_{sig}$   
 $X_{C2}(\omega)$  = the reactance of the capacitor  $C_2$

The noise voltages and currents are random, so their value as a function of time or of frequency cannot be completely determined. What can be specified is the average noise power, or the power spectral density of the noise. Power spectral densities represent the magnitude squared of the voltage, current or other parameter, as a function of frequency per unit bandwidth.

If we assume that the noise sources are not correlated with each other (noise sources that derive from independent mechanisms will satisfy this condition), then the noise power spectral density at the amplifier input is given by:

$$\begin{aligned} S_{V_a}(\omega) &= |V_a(\omega)|^2 / \text{bandwidth} = V_a^*(\omega) \cdot V_a(\omega) / \text{bandwidth} \\ &= S_{V_{na}}(\omega) + S_{I_{na}}(\omega) |Z_m(\omega)|^2 + (S_{V_{sig}}(\omega) + S_{V_{nt}}(\omega)) \left| \frac{X_{C2}(\omega)}{Z_l(\omega)} \right|^2 \end{aligned}$$

where \* represents the complex conjugate operator.

More importantly than the noise power spectral density presented to the amplifier input, is the ratio of the noise terms to the signal term (NSR) as seen by the amplifier input. This is given by:

$$\text{NSR} = \frac{1}{S_{V\text{sig}}(w)} \left( S_{V\text{nt}}(w) + \left| \frac{Z_l(w)}{X_{C2}(w)} \right|^2 \left( S_{V\text{na}}(w) + S_{I\text{na}}(w) |Z_m(w)|^2 \right) \right)$$

If we define two different variables to characterize the amplifier, through an optimum noise impedance and noise power:

$$R_{\text{opt}} = \sqrt{\frac{S_{V\text{na}}(w)}{S_{I\text{na}}(w)}}, \text{ and } P_{\text{opt}} = 2 \sqrt{S_{V\text{na}}(w) S_{I\text{na}}(w)},$$

then the noise to signal ratio can be re-cast to the form:

$$\text{NSR} = \frac{S_{V\text{nt}}(w)}{S_{V\text{sig}}(w)} + \frac{1}{2} \left( \frac{R_{\text{opt}}}{|Z_m(w)|} + \frac{|Z_m(w)|}{R_{\text{opt}}} \right) P_{\text{opt}} \left( S_{V\text{sig}}(w) \left| \frac{X_{C2}(w)}{Z_l(w)} \right|^2 \frac{1}{|Z_m(w)|} \right)^{-1} \quad [1]$$

The first term represents the Nyquist noise voltage term arising from the pickup coil. This means the Nyquist noise in the coil represents a broadband detection sensitivity limit, even if the amplifier produced zero noise. The pickup coil would still limit the detection performance of the system. The second term in the NSR calculates the ratio of the amplifier noise power to the applied signal power. Although this expression looks complicated, it can be broken down into several parts.

The first part of the amplifier contribution (i.e., the first term in parentheses) is a scale factor showing how closely the circuit impedance (seen from the amplifier) matches the optimum noise impedance of the amplifier. The amplifier has a quadratic minimum in its noise performance when the circuit's source impedance matches the amplifier's optimum noise impedance. When multiplied by  $P_{\text{opt}}$ , this then represents the noise performance of the amplifier when connected to an input impedance of  $|Z_m(w)|$ .

The second part of the amplifier noise contribution (the final term in parentheses) calculates how much of the signal's voltage spectral density appears across the amplifier input, when applied to the voltage divider formed between the reactance of  $C_2$  and the total loop impedance.  $S_V(w)$  has units of  $\text{volt}^2/\text{Hz}$ , hence the square in the impedance ratio. When this is divided by  $|Z_m(w)|$ , it represents the signal power applied to the amplifier input.

### 3.3.1.1 Practical Implications of the Noise Analysis

The noise to signal ratio expression in equation 1 above shows two separate noise contributions. First, there is the detection limit from Nyquist noise of the pickup coil, which is virtually independent of frequency over the bandwidths of interest for NQR.

And second there is the amplifier noise contribution, which is strongly frequency dependent owing to the reactance of the matching elements.

The current generation of NQR explosives detection electronics employs room temperature (290 K) pickup coils and amplifiers (with noise temperatures of approximately 100 K). At the center of resonance the 290 K thermal noise from the pickup coil dominates, so for signals centered on this frequency there would be little benefit from quieter amplifiers. However, when the system tries to detect signals away from the center of resonance, the frequency dependent impedance of the matching elements decreases the coupling of the amplifier to the pickup coil. As the signal is moved from the center of resonance, the amplifier noise performance will start to dominate over thermal noise of the pickup coil.

Thus, for significantly improved broadband detection of NQR signals, both the coil and the amplifier should be optimized. In addition, for a given pickup coil and amplifier one can optimize the matching circuit depending on the desired system bandwidth. The fundamentals of these techniques are described below.

### **Improvements to the Pickup Coil**

If the pickup coil is optimally matched to the amplifier, the amplifier will see only the resistive losses in the coil at the resonant frequency. Thus at resonance, a pickup coil at 290 Kelvin will present 290 Kelvin of thermal noise to the amplifier. The noise power spectral density of the Nyquist noise voltage is given by  $S_{V_{nt}} = 4 k T R_t$ , where  $k$  is Boltzman's constant,  $T$  is absolute temperature of the dissipative element, and  $R_t$  is the effective series resistance of the coil. For a given coil inductance, there is a clear advantage in signal to Nyquist noise ratio by maximizing the  $Q (= \omega L/R)$  of the circuit. Increasing the  $Q$  directly decreases  $R_t$  and hence the Nyquist noise voltage. There is also a clear advantage in cooling the coil, which reduces both  $T$  and  $R$ . Cooled sensors are now commonly used in many military applications (e.g. infrared imagery). Cooling the NQR pickup coil seems to be an obvious way to improve the system detection performance.

### **Improvements to the Amplifier**

There are many different measures of the noise performance of an amplifier, but in this case a good metric is the noise temperature of the amplifier. This figure specifies what temperature a resistor must be, so that when it is connected to the amplifier's input the amplifier adds the same amount of noise during the measurement process as the noise coming from the resistor itself. Another way of expressing this is to consider the noise coming from the resistor to be the signal one is trying to detect. An amplifier with a noise temperature equal to the resistor's temperature will be able to detect the resistor signal with unity signal to noise ratio.

There are a number of semiconductor devices that have noise performances significantly better than the 100 K transistors used in the current generation of NQR scanner products (for example, a bipolar NPN RF signal transistor). The noise figure for a Motorola MRF571 falls with frequency, and is 0.6dB at 150 MHz. It seems reasonable to expect this fall in the noise would continue below 0.5dB at several MHz, which corresponds to a noise temperature of 35 Kelvin.

There are also more exotic devices, such as MESFETs, that have noise performances at 4MHz at the sub-Kelvin level when cooled to 77K. If the noise from the pickup coil were to be reduced by cooling the coil, then cooling an amplifier would not present any logistical difficulties, and could significantly improve the detection sensitivity and bandwidth. MESFETs have much higher optimum noise impedances that must be matched, which would require changes to the system design but do not (in principle) pose a problem.

As discussed in the Phase I proposal, for the ultimate in noise performance the front end amplifier can be replaced with a SQUID. When used as an RF amplifier, a SQUID's effective noise performance is directly proportional to the signal frequency. At 93 MHz a DC SQUID has been measured to have a noise temperature of 1.7 Kelvin<sup>iv</sup>. Scaling the frequency down to the detection frequencies of RDX and PETN explosives, shows a SQUID to have a noise temperature of several tens of milli-kelvin. In addition, SQUIDs have very low input impedances, making matching to the coil much simpler.

### **3.3.2 Improved Impedance matching networks**

An alternative approach to improving the bandwidth of the system relies not on finding a quieter amplifier, but instead on designing the network that matches the impedance of the pickup coil the amplifier to stay close to matching the optimum noise impedance of the amplifier over a broader frequency range.

The greatest impediment to optimum signal transfer from the pickup coil is the reactance of the coil. At a single frequency, a simple series resonant capacitor is sufficient to remove this inductive reactance and leave only the resistive component of the coil. Unfortunately, a high Q resonant system gives a very narrow region over which the impedance of the coil is dominated by the resistive component, resulting in a very narrow effective detection bandwidth.

It is possible to use feedback techniques to flatten the response of a resonant system, but it can be shown in general that this does nothing to improve signal to noise ratio of a system (at least in linear systems). Adding series resistance could also broaden the resonance, but at the cost of adding noise. In fact, the result is to worsen the sensitivity of the system at the center of resonance, increasing the bandwidth only in the sense of producing a system where there is a wider frequency range before the amplifier noise gets as bad as this worsened Nyquist noise.

To truly improve receiver bandwidth more sophisticated techniques it must be used, and each optimized for the bandwidth of interest. Under this program, three advanced techniques were considered.

**Noise Impedance Matching.** In general, the best noise performance of an amplifier is obtained when the source impedance of the signal matches the amplifier's optimum noise impedance. This optimum noise impedance is defined by the square root of the ratio of the amplifier's voltage noise power spectral density (PSD) to the amplifier's current noise PSD. In the case of NQR detection, the source impedance is the impedance of the pickup coil and matching network components (series and parallel capacitors) as seen from the amplifier input. The best signal transfer will be when the reactive components in the input circuit impedance have been canceled out and the impedance seen is the transformed resistive loss in the coil. The best signal to noise ratio will be when the transformed resistive loss matches the optimum noise impedance. However, the match can only occur at resonance and exhibits a relatively strong dependence on frequency away from resonance.

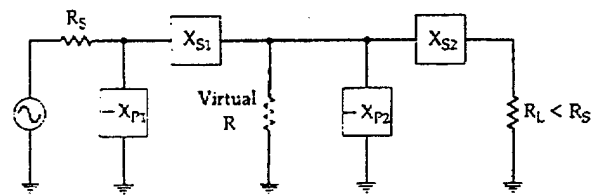
**Bandwidth Optimized Overcoupling.** One can make the resistive losses in the coil less than the optimum amplifier noise impedance. This is equivalent to making the coil  $Q$  too high, or "overcoupled". The SNR at resonance is reduced but the response is less frequency dependent away from resonance than for a noise impedance match. Thus, although the peak noise performance is worse, the overall noise performance (when averaged over a specific bandwidth) is higher. We wrote a computer program to optimize the average performance by a process of least squares iteration.

**Dual Resonant Matching.** What we fundamentally require is a matching network that removes the reactance of the pickup loop, but whose impedance deviates less rapidly from the center of resonance than of a single, high  $Q$  resonant circuit. This can be achieved by designing the system to be multiply resonant, having a set of closely spaced resonances close to the detection frequency. A mechanical analog to this is the action seen in coupled mechanical oscillators. The interaction between the oscillators forms a system with 'normal-mode' frequencies that are split up and down from the original resonance frequency. The impedance at a center of resonance will be at a local extremum (either a maximum or minimum depending on whether we are coupling in series or parallel) and will deviate from this extremum as the center of resonance is deviated. If, however, the system has multiple resonances, the impedance of the next resonance will start to dominate as the previous resonance is departed. By a careful choice of the frequency splits between the two resonances, a broad region can be formed where the impedance of the circuit does not deviate too much from matching the optimum noise impedance of the amplifier. This technique allows a broadened match.

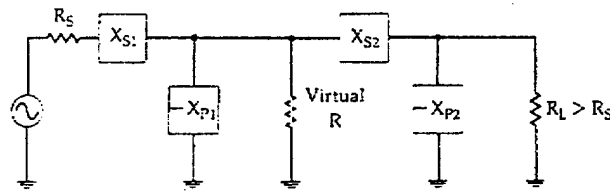
Shown in Figure 8 is an extract from a standard work on RF design<sup>v</sup> showing coupled resonant networks used to achieve wide band frequency matching. (The  $X_s$  and  $-X_p$  elements represent the reactance of series inductors and shunt capacitors.) We considered a number of different circuit designs for the dual resonant matching circuit. A problem

with the general type of circuit shown in Figure 8 is that to achieve resonances which are very close together, one must use very different values for capacitors and inductors in the first and second stages. One way to overcome this is to use a transformer to weakly couple the two resonant oscillators. In the calculations presented in the following section, the separation of the two resonances was optimized as a separate free parameter using computer-based least squares iteration.

A disadvantage of the dual resonant approach, in general, is that the second resonant circuit entails additional system size and weight. This probably rules out the dual resonant approach for a practical mine detection system. However, the results were calculated for completeness to put in perspective the use of a SQUID which is probably the ultimate amplifier at these frequencies.



(A) *R in shunt leg.*



(B) *R in series leg.*

Fig. 4-25. Two series-connected L networks for lower Q applications.

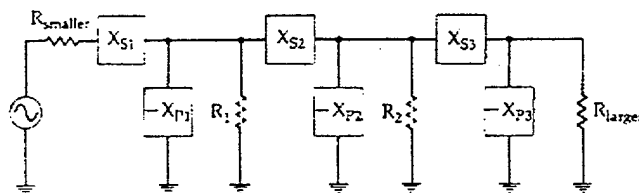


Fig. 4-26. Expanded version of Fig. 4-25 for even wider bandwidths.

## Figure 8. Multiple Resonant Networks for Broadband Impedance Matching

### 3.3.3 Results of Mathematical Calculations Using the Model

The physical and mathematical model for NQR detection has been programmed into a computer so that it may be used to rapidly predict the performance of the alternative transistor and SQUID detection circuit designs. The parameter space for the entire



system is very large, and in order to simplify the comparisons we fixed the pickup coil dimensions at 15 cm radius with an inductance of 683 nH.

To further reduce the problem, a total of four fundamental circuit design strategies were defined. A brief description summarizing each approach is given below. In comparing them, each approach was optimized to produce the lowest overall system noise of the specified bandwidth.

Noise Impedance Match: matching the amplifier to the sample coil so that the real impedance of the sample coil as seen by the amplifier is equal to the *noise impedance* (the ratio of voltage noise to current noise, not the measured input impedance) of the amplifier. The NIP can only be exact at resonance and gives the best signal to noise ratio at resonance.

Bandwidth Optimized: equivalent to the overcoupling technique used occasionally by researchers in NQR. Although the noise performance at resonance is actually worse, an overall noise performance when averaged over a specific bandwidth is improved. The optimization is done by computer iteration..

Optimized Dual Resonant: the same as *Bandwidth Optimized* except that a coil with two resonant frequencies is used. Both the frequency separation of the double resonance and the amplifier coupling are optimized.

HTS SQUID: a high temperature superconductor (HTS) SQUID of current design, which is matched directly to the sample coil at the resonant frequency using a superconducting transformer

To get an easy-to-interpret mental picture of the different designs it is convenient to specify the bandwidth over which to compare them. In fact two of the transistor-based designs require optimization over a chosen bandwidth. There are many possible measurement advantages offered by wider bandwidth detection sensitivity, such as the detection of closely spaced multiple spectral lines in the target substances, the discrimination of spurious signals in the region of the pickup coil, and the detection of substances with very rapid NQR decay times.

The bandwidth of the detection system is a somewhat arbitrary concept, because it requires us to define how far the sensitivity must drop before we declare the edge of the detection band. Typically we want a detection system to be as sensitive as possible. So, a reasonable definition of the edge of the detection band is where the detection sensitivity has dropped by a small amount (say 3dB) from the system's peak detection sensitivity. Considering these points, we decided to bracket the specific detection bandwidths (at 3.4 MHz) of interest as follows:

<u>5 kHz</u>	Absolute minimum to get signal discrimination from acoustic ringing at 3.41 MHz
<u>10 kHz</u>	Same as 5 kHz but with sufficient additional bandwidth to allow for 50°C of ground temperature variation
<u>25 kHz</u>	Equivalent to 6.5 kHz at 890 kHz, adequate to detect PETN with signal discrimination.
<u>60 kHz</u>	Adequate to detect two lines of RDX simultaneously. Equivalent to 16 kHz at 890 kHz, providing around 100 °C of temperature shift for PETN or the possibility to detect 6 spectral lines of TNT
<u>125 kHz</u>	Three lines of RDX; PETN + 6 lines of TNT
<u>1 MHz</u>	Arbitrary definition for extreme broadband detection

The predictions for semiconductor and SQUID preamplifiers connected to the antenna at various temperatures and quality factor, are given in Table 2, Table 3, and Table 4. The entries in the tables represent the relative measurement time needed to achieve the same detection signal to noise ratio; a shorter measurement time is desirable. For comparison, all results are divided by the Nyquist (Johnson) noise of the detection coil when the coil temperature is at 77K and  $Q = 1000$ . To aid in understanding the results, the reader should be aware of the following general synonyms and principles:

More System Noise  $\Rightarrow$  Lower Detection Sensitivity

More System Noise  $\Rightarrow$  Longer Measurement Time

Greater Bandwidth  $\Rightarrow$  Lower Detection Sensitivity

Higher  $Q$   $\Rightarrow$  Lower System Noise

Lower System Temperature  $\Rightarrow$  Lower System Noise

In Table 2 we compare the different techniques for a room temperature pickup coil with a conservative  $Q$  of 200. The noise temperature of the transistor used for the three semiconductor approaches is 100K (the physical temperature is 300K).

**Table 2. Comparative of Relative Measurement Time for Three Optimized Transistor Techniques and an HTS SQUID. Pickup coil temperature, 300K; transistor noise temperature, 100 K,  $Q = 200$ .**

	5 kHz	25 kHz	60 kHz	125 kHz
Noise Impedance Match	26.1	28.2	39.1	83.1
Bandwidth Optimized	26.1	28.0	34.1	47.5
Optimized Dual Resonant	26.2	27.9	30.8	39.4
High Tc SQUID	19.6	19.6	19.9	20.9

We see that the *noise impedance match* does indeed give the lowest measurement time (highest sensitivity) at low bandwidths for transistor amplifiers. The low noise, coupled with the fact that it is the easiest to optimize, is why the NIP is by far the most commonly used technique in magnetic resonance. However, we see that the more sophisticated techniques of optimized single and dual resonant circuits offer substantial speed enhancements over the NIP at larger bandwidths. For broadband detection the advanced transistor techniques are around a factor of two faster. We also see that even for the low  $Q$  room temperature antenna, the HTS SQUID preamplifier is almost a factor of two faster than the best conceivable transistor system.

In Table 3, we compare the same four fundamental pre-amplifier designs when used with what is probably the best antenna that could be built for mine detection using current technology. The general result is that when the coil produces less noise, the effect of the amplifier on the overall performance is much greater. For example, the "standard" noise impedance match requires 101 times more time to make the measurement in a 125 kHz bandwidth, as compared to 83 times for the higher noise antenna (Table 2).

**Table 3. Comparison of the Relative Measurement Time for The Alternative Techniques when Used with Cooled Electronics. Antenna temperature, 77K; transistor noise temperature, 35 K;  $Q = 1000$ .**

	5 kHz	25 kHz	60 kHz	125 kHz
Noise Impedance Match	1.61	5.75	24.5	101
Bandwidth Optimized	1.59	2.96	5.60	10.5
Optimized Dual Resonant	1.60	2.54	4.28	7.60
High Tc SQUID	1.04	1.08	1.27	1.49

From Tables 2 and 3 we see that the Bandwidth Optimized, Optimized Dual Resonant and High Tc SQUID all offer substantial improvements over the current state-of-the art in receiver design when a even a small fractional bandwidth (25 kHz = 0.7%) is required. The Optimized Dual Resonant is considerable more complex and bulky to implement than the Bandwidth Optimized approach, which the same physical size as the conventional Noise Impedance Match. The HTS SQUID is in a class of its own. We therefore take as our two candidate techniques the Bandwidth Optimized and HTS SQUID.

In Table 4 we compare these two approaches at two extremes of bandwidth with different antennas of differing performance. For simplicity we have used the optimum transistor temperature of 35 K for the Bandwidth Optimized scenario.

**Table 4. Comparison of Bandwidth Optimized Cold Transistor with an HTS SQUID for Various Pickup Coil Temperatures and Quality Factors.**

	Band. Opt. 10 kHz	Band Opt. 125 kHz	HTS 10 kHz	HTS 125 kHz
<b>T = 300, Q = 200</b>	26.3	83.1	19.6	20.9
<b>T = 200, Q = 500</b>	6.39	14.9	5.25	5.68
<b>T = 77, Q = 500</b>	3.18	11.56	2.05	2.49
<b>T = 77, Q = 1000</b>	1.88	10.5	1.04	1.49

Again, we see the same general trends: the quieter amplifier has more effect when higher bandwidths are required, and a quieter antenna is used. To proceed further with our analysis in order to make a final decision regarding the choice of amplifier, we need to determine the required bandwidth and the Q that can be expected from the antenna. Both of these question require further investigation of the mine detection problem per se from the perspective of NQR.

To summarize, we see that our current NQR technology, which is actually state-of-the-art, will be totally inadequate to be operated in broadband mode. Development of a cooled semiconductor system would represent a major improvement, but may still be too insensitive to use if a very broadband mode were required. The SQUID preamplifier, however, has almost the same sensitivity in narrow-band and broadband mode, and would provide a significant improvement over all alternative techniques.

### 3.4 Task 4: Phase I Option Task: Engineering Design

This task is scheduled for the Phase I Option period, but we have already had numerous scientific and programmatic discussions in light of the expansion of our overall NQR mine detection effort. In particular, many specific goals of the engineering design have been advanced in light of the awarding of a DARPA-funded program to develop a two compound (TNT & RDX) detection system. Under the DARPA program we will focus on detecting TNT, which is a difficult problem. Significant additional measurement capability will be developed under the DARPA-funded program. This will make it possible to utilize more advanced NQR techniques for detecting RDX, such as measuring two spectral lines instead of one.

Thus, in Phase I of this program it would be premature to finalize specific design parameters such as the system operating frequency, which were to be defined under this task. By the same token, the Phase II SBIR program will now contain several new challenges that were not present when we intended to build a system to detect only RDX. Accordingly, we have extended Task 4 to consider the following new issues:

Metal Detection. We will identify and compare alternative design modifications to the proposed single sided NQR system in order to detect metallic cased landmines. This task will involve simple laboratory measurements to confirm the calculations and predictions.

PETN Detection. We will identify potential design modifications that must be made to a TNT/RDX NQR system to accommodate the detection of the high explosive PETN, which is the third most common constituent of landmines.

In keeping with the spirit of an SBIR Phase I program, these items are intended to assess the feasibility of the technical modifications and to discuss alternative strategies, which could be used as backup approaches if difficulties are encountered. The actual hardware and software design to implement PETN and metal detection will be carried out in Phase II.

## 4. Summary

We have successfully addressed the Phase I technical tasks. A number of important facts relating to the feasibility of detecting mines by NQR have been ascertained. These may be summarized as follows:

- 1) Distribution of mines by type of explosive material. We believe that NQR-based techniques will be able to detect around 90% of all plastic cased mines. With the addition of algorithms to distinguish metal, it should be possible to detect 90% of all mines, and a similar fraction of UXO.
- 2) Man portability. A study of the power and weight issues in NQR indicates that a truly man portable system is feasible.

- 3) Signal Processing. A preliminary study of several alternative signal processing techniques indicates that it is possible to reduce the current NQR false alarm rate by a significant amount.
- 4) Preamplifier Design. A group of new amplifier designs have been considered which offer substantial improvements in system bandwidth over current narrow-band techniques.

With the start of a parallel program to develop the capability to detect landmines via their TNT content, this SBIR program has the possibility of providing to the Marine Corps a prototype landmine detection system with high sensitivity to all types of mine.

## 5. References

---

<sup>i</sup> Regina E. Dugan, bidders background information supplied by DARPA on *Detection of Landmines and Unexploded Ordnance*, June 1996.

<sup>ii</sup> *Minefacts*, an interactive CD-ROM developed by the US Department of Defense, Office of Humanitarian and Refugee Affairs, 2500 Defense Pentagon, Washington DC. And technical information on mine types and composition supplied to QM by Lt. Col. W. Macecevic, US Marine Corps.

<sup>iii</sup> A "Threat Quantity" is the amount of explosive deemed by the FAA to be sufficient to bring down a commercial airliner. It is a classified quantity.

<sup>iv</sup> C. Hilbert and J. Clarke, *DC SQUIDS as Radiofrequency Amplifiers*, J Low Temp. Phys., **61**, 263 (1985).

<sup>v</sup> C. Bowick, *RF Circuit Design*, Prentice Hall, 11711 North College, Carmel, IN.